Korean J. Chem. Eng., 39(11), 3092-3101 (2022)
DOI: 10.1007/s11814-022-1177-1

pISSN: 0256-1115
eISSN: 1975-7220

A new antifouling metal-organic framework based UF membrane for oil-water separation: A comparative study on the effect of MOF (UiO-66-NH_2) ligand modification

Mahya Samari*, Sirus Zinadini*,,†, Ali Akbar Zinatizadeh*,**, Mohammad Jafarzadeh***, and Foad Gholami***

*Department of Applied Chemistry, Faculty of Chemistry, Razi University, Kermanshah, Iran
**Environmental Research Center (ERC), Department of Applied Chemistry, Faculty of Chemistry, Razi University, Kermanshah, Iran
***Department of Organic Chemistry, Faculty of Chemistry, Razi University, Kermanshah 67149-67346, Iran
(*Received 29 January 2022 • Revised 11 May 2022 • Accepted 14 May 2022*)

Abstract−Surface-modified metal-organic frameworks (MOFs) were used for the fabrication of polyethersulfone (PES)-based polymeric composite membranes by phase inversion method. Initially, zirconium-based MOF, UiO-66-NH_2, was modified with melamine (denoted as UiO-66-NH-Mlm) and ethylenediamine (UiO-66-NH-EtNH_2) via a solvothermal post-modification technique. The fabricated polymeric membranes were then employed for oil-water separation and showed satisfactory hydrophilicity and antifouling performance (PWF: 55.38 kg/m^2·h, FRR: 90.67 %, Rr: 46.94%, Rir: 9.33% and >99% rejection to the oil). It was due to the formation of the hydration layer, arising from the available -NH_2 groups (providing hydrogen-bonding) on the surface of the modified MOFs (WCA: 51.66°), and the lower surface roughness. Higher hydrophilicity and better antifouling efficiency were obtained for the membranes using UiO-66-NH-Mlm, compared to UiO-66-NH-EtNH_2, due to the higher number of -NH_2 groups. The membranes also exhibited good thermal stability owing to the fine dispersion of the modified MOFs in the polymeric texture and the presence of metallic cores in the MOFs. The membranes were also applied for frequent filtrations with great performance.

Keywords: Flat-sheet Membrane, Long-term Performance, Ultra-filtration, UiO-66-NH_2, Oily Wastewater

INTRODUCTION

At this precise moment, environmental pollution by filtering and repulsing residuum has become one of the biggest problems of civic aquarium ecosystems across the world. The dangerous factors in these systems are varied adequate and involve emerging pollution (fly dopes, herbicides, pest management poisons and remaining), and also many known harmful chemicals such as volatile organic compounds (VOCs), polyaromatic compounds (PAHs), persistent organic pollutants (POPs) and low concentration of oily compound [1]. Frequent marine incidents of oil leaks and oil pollution caused by fast industrialization have made intense problems for aquatic systems and human health. Thus, this kind of oil pollution has been turned into one of the biggest environmental concerns [2-4]. Marine sources are very vulnerable to this human calamity, such as the Exxon Valdez Oil Spill in Alaska, which did hideous damage to nearly 300,000 living creatures and the ecological effects are still continuing [5]. Therefore, in research and industrial societies the detachment of oil from the water has become a new topic. Current counteractions in oil leak incidents include pollution analysis with chemical materials, in-place burn, and vacuum suction [6,7]. Nonetheless, it has been proved that all these methods are expensive and partly inefficient, even causing second pollution. More importantly, a selective oil-water separation for recovery of precious oil resources has gained interest. So, expansion of materials that could disport oil-water combination selectively, efficiently, and eco-friendly is necessary. Considerable efforts in the research field have been done [8]. In recent years, the development of specific materials with high ability as water-absorbent has become a new topic in materials research. It is believed that special ingredients with opposed nature to oil and water is the most hopeful material (e.g., hydrophilic material) for selective oil-water detachment [9,10]. Theoretically, wettability actions are telling off by surface chemistry and it can be amplified by surface structure [8]. In fact, most published progressive material with special ingredients can be used for elective oil-water separation, showing a synergistic phenomenon between surface chemistry and architecture.

Conventional membranes have many benefits, such as low cost, acceptable efficiency for a virus, organic macromolecules, colloidal pollutant, and applicable filtration and recycling of sewage [11,12]. In contrast, some different issues have arisen, for example, poor mechanical strength, low anti-fouling ability, low durability for long-term filtration, and requiring frequent clean-up and membrane replacement. Due to short porous channels in the membranes, it requires a large amount of energy (transmembrane pressure) for membrane recovery [13,14]. Yet ultrafiltration membranes are not capable of eliminating low concentration pollution, which is a major polluter in sewage. To work out this concern, the next generation of multi-function membrane technologies has been developed [15, 16]. Recent reports have showed that by using new filler for modi-

†To whom correspondence should be addressed.
E-mail: sirus.zeinaddini@gmail.com

fication of the polymeric membranes, e.g., TiO_2 [17], carbon nanotubes (CNT) [18], covalent organic framework (COF) [19], mesoporous [20]. C_3N_4 [21], metal-organic framework (MOF) [22,23], and graphene [24]. This issue can be solved. A selective separation will be achieved for oil-water emulsion because special ingredients allow only one phase (water) to penetrate. Therefore, polymeric membranes with lower and controllable porosity still have unique benefits for an oil-water mixture. By reforming polymeric membranes with special wettability (and anti-fouling ability, high flux, perfect refinery efficiency), filtration will be significantly improved [25].

In the last decade, MOFs which consist of metallic cores and organic ligand bridges have attracted attention as a fitting platform for guest-host chemistry [26]. The solid materials are being before other current porous materials [27]. Some incredible virtues such as high chemical stability (stable structure and good linkage), uniform and adjustable pores, very high variety, and geometry in structures with many different metallic ions and ligands, are notable. These properties result in many benefits for modified membranes compared to un-modified membranes [28]. Although the MOFs have wide usage in the separation and absorption of gas, their applications in liquid separation have only been developed recently [29]. The performance of the fabricated modified membranes by introducing MOF to the membrane matrix was significantly increased. In these membranes, a polymer is offering a continuing phase, while MOF particles with unique features (e.g., hydropathic, high porosity, chemical stabling) act as a heterogeneous phase [30].

In 2019, Liu and coworkers used mesoporous hybrid PAV/SiO_2 nanoparticles in PVDF membrane for efficient simultaneous elimination of oil pollution and heavy metals, resulting in anti-fouling ability, high flux, and acceptable efficiency in heavy metal removal (e.g. copper) [20]. Gholami et al. studied the anti-fouling property and oily wastewater rejection by adding Zn-based MOF (TMU-5) to the PES polymer membrane [21]. Due to the hydrophilic nature of nanoparticles in the membrane matrix, excellent hydrophilic and anti-fouling properties have been achieved. [22]. Lee et al. introduced a direct osmosis membrane for filtration of oily wastewater, which is made by the thin-film composite (TFC) method by employing poly[3-(N-2-methacryloylxyethyl-N, N-dimethyl)-ammonatopropanesulfonate] (PMAPS). The results showed high flux and low fouling for oily wastewater, and 95% efficiency for oil emulation [25]. Zarghami and co-workers introduced that by polymerization of dopamine in the PES membrane, the flux is significantly improved with good self-cleaning and anti-fouling properties (efficiency >98%) [31]. The filler of the ZnO microsphere/carbon nanotube has also shown high rejection, good flux, and long-term stabilizing [32]. Moreover, zwitterionic nano hydrogel-grafted PVDF (ZNG-g-PVDF) based membrane has exhibited high anti-fouling quality and high oil rejection for a very low concentration of oil pollution (13 ppm) [33].

In our previous work, the melamine-modified UiO-66-NH_2 was used for the PES-based membrane and showed high performance in oily wastewater separation compared to that using the unmodified UiO-66-NH_2 [34]. In the current work, we introduce MOF-based membranes using UiO-66-NH_2 modified with melamine and ethylamine. For enhancement of the oil rejection efficiency, the modification of the MOF is carried out in a solvothermal method to obtain higher loadings of the organic modifiers (i.e., melamine and ethylamine). The characteristics of the membranes are investigated with electron microscopy, surface topography, water contact angle, pure water flux (PWF), flux recovery ratio (FRR), and long-term filtration.

MATERIAL AND METHODS

1. Materials

Polyethersulfone (PES; glass transition T_g=225 °C, average molecular weight=58,000, Ultrason E6020p) as the main polymer was purchased from BASF (Germany); dimethylacetamide (DMAc; BASF company) as the solvent, and polyvinylpyrrolidone (PVP; molecular weight=25,000 g mol^{-1}) as pore maker was supplied from Merck (Germany); $ZrCl_4$, 2-aminoterephthalic acid, chloroethylamine hydrochloride, cyanuric chloride NH_3, $CHCl_3$, DMF, and EtOH were purchased from Merck in analytical grade. In all experiments, distilled water was applied.

2. Preparation and Modification of UiO-66-NH_2

2-1. Preparation of UiO-66-NH_2

The preparation of UiO-66-NH_2 was adopted from the reported method [35]. In the first vial, $ZrCl_4$ (0.54 mmol) was added to the mixture of DMF (5 mL) and HCl (10%, 1 mL), and the mixture was sonicated for 25 min. In the second vial, 2-aminoterephthalic acid (0.75 mmol) was dissolved in DMF (10 mL) under sonication. The content of the two vials was mixed, sonicated for 20 min, and heated in an oven (at 80 °C) for 24 h. The precipitate was separated by centrifugation, washed several times with DMF and ethanol (Merck), and activated in an oven at 120 °C for 24 h.

2-2. Solvothermal Modification of UiO-66-NH_2 with Ethylamine (UiO-66-NH-EtNH_2)

0.1 g UiO-66-NH_2 was dispersed in 6 mL $CHCl_3$ and sonicated for about 5 min. 2-Chloroethylamine hydrochloride (0.013 g) was added to the mixture and stirred at 60 °C for 24 h. To neutralize the generated HCl in the first stage of the modification, which may form ammonium chloride, NH_3 was added to regenerate amine groups. NH_3 (0.12 mmol) was inserted into the mixture, and stirring continued for 24 h at 60 °C. Finally, the resulting solid was centrifuged, washed with $CHCl_3$ (3 times) and methanol (3 times), and dried at 150 °C for 5 h.

2-3. Solvothermal Modification of UiO-66-NH_2 with Melamine (UiO-66-NH-Mlm)

0.1 g UiO-66-NH_2 was dispersed in $CHCl_3$ (6 mL) by sonication for 5 min. To the mixture, cyanuric chloride (0.022 g) was added, and the temperature was set at 60 °C for 24 h stirring. NH_3 (0.12 mmol) was then added to the mixture and stirring continued for 24 h by controlling the temperature at 60 °C. The solid sediment was separated by centrifugation, washed with $CHCl_3$ and methanol several times, and dried at 150 °C for 5 h.

3. Fabrication of Mixed Matrix MOF-based Membrane

Flat sheet asymmetric porous membranes were fabricated with modified MOFs by applying a phase inversion method. The casting solutions were prepared by mixing different quantities stated in Table 1. For example, an appropriate amount of additives was dispersed in DMAc by sonication (DT 102 H bandeling ultrasonic,

Table 1. The composition of casting solution for the fabrication of the membranes (bare and embedded membranes)

Membrane type	PES (wt%)	PVP (wt%)	DMAc (wt%)	Modified MOF (wt%)
M_1	17	1	82	-
M_2	17	1	81.9	0.1[a]
M_3	17	1	81.5	0.5[a]
M_4	17	1	81.9	0.1[b]
M_5	17	1	81.5	0.5[b]

[a]UiO-66-NH-Mlm
[b]UiO-66-NH-$EtNH_2$

Germany) for 25 min. PVP and PES were introduced to the mixture and stirred (400 rpm) for 24 h. For homogeneity of the casting solution, a sonicated-assisted method was used to remove all air bubbles. For the purpose of membrane fabrication, a film applicator (150 μm thickness) and a neat glassy plate were applied for casting. The cast plate was promptly immersed in a distilled water tank. After the formation of the solid polymeric membrane, it was transferred to a new distilled water tank overnight to ensure phase inversion completely occurred. The obtained membrane was stored in filter papers to dry under ambient conditions (~24 h).

4. Characterization of MOF-based Membrane Morphology

X-ray diffraction (XRD) was applied to study the structure of the additives (by a Rigaku D-Max C III diffractometer (Cu Kα, λ=1.5418 Å)). The surface functionality of the MOFs was investigated by attenuated total reflection (ATR)-infrared spectroscopy (Perkin Elmer UATR). CHNSO elemental analyzer (Euro EA-HEKAtech GmbH) was used for elemental analysis under N_2 gas flow. Thermogravimetric analysis (TGA) was used (model: Linseis STA PT-1000) to estimate the loading of ethylamine and melamine on the surface of UiO-66-NH_2 (using nitrogen flow and heating rate of 20 °C min^{-1}). The data of BET surface area and pore size/volumes were obtained by applying a porosimeter NOVA 2200e at 77 K.

To evaluate the characteristics of the membranes, a scanning electron microscope (SEM; Philips-XL30, The Netherland) was applied with an acceleration voltage of 20 kV. For sampling, a small piece of the membrane was initially frozen by liquid nitrogen and then sputtered by gold. Atomic force microscopy (AFM; Nanosurf® Mobile S scanning probe-optical microscope, Switzerland) was used to study the topography of the membrane surface. The difference between peaks and valleys is defined as surface roughness, and a smoother surface has fewer differences. Other parameters such as S_a (average roughness), S_q (the root of two data), and S_z (the average data between the lowest valley and the highest peak) can be also obtained by AFM. The membrane water tendency was quantified by a water contact angle (WCA) measurement. Low contact angles between membrane surface and water droplet indicate a more hydrophilic nature. For this purpose, a small droplet of distilled water was injected (4 μL) onto the surface of the clean membrane. After waiting for 10 seconds, to face stable conditions, a digital microscope (Contact Angle meter XCA-50) captured the images, and the CA was then calculated. For obtaining reliable results, the test was repeated five times and the average value was reported.

5. Porosity Measurements of the Membranes

To measure the porosity of the membranes, a gravimetric method was applied. First, a small piece of a membrane (4 cm^2) was cut and weighed precisely. Then, the weight of the sample was measured after submerging the sample into distilled water for 24 h. According to Eq. (1), the membrane porosity was calculated:

$$\varepsilon = \frac{\omega_1 - \omega_2}{A \times L \times dW} \tag{1}$$

where ω_1 and ω_2 are the wet and dry weights of membranes, respectively. A, L, and dW are effective surface, membrane thickness, and water density (998 kg/m^3), respectively.

6. Membrane Setup and Performance

To consider the membrane performance, all the fabricated membranes were evaluated in a 150 mL dead-end setup, which was made of stainless steel [34]. The effective membrane surface was 12.56 cm^2. The setup was equipped with a nitrogen flow to assist the feed passing through the membrane. Stirring was applied to reduce the feed polarization to a minimum. The membranes were examined at 3 bar and the data were recorded after a steady state.

By using a gravimetric method, the PWF was calculated:

$$J_{w.1} = \frac{M}{A\Delta t} \tag{2}$$

where M (kg), A (m^2), ΔT are defined as permeate weight, membrane effective area, and filtration time (h), respectively.

7. Fouling Effect

For this purpose, a milk powder solution was selected as a proper foulant. The membrane was first evaluated by distilled water under 3 bar pressure for 60 min, then milk powder solution (1,000 ppm) was applied under the same conditions for 90 min. Finally, the membrane was tested again with distilled water for 60 min. The flux recovery ratio (FRR), defined as membrane resistivity against fouling, was obtained according to Eq. (3):

$$FRR = \left(\frac{Jw2}{Jw1}\right) \times 100 \tag{3}$$

Different types of fouling, such as total fouling ratio (R_t), reversible fouling ratio (R_r), and irreversible fouling ratio (R_{ir}), were also calculated:

$$R_t(\%) = \left(1 - \frac{j_p}{j_{w.1}}\right) \times 100 \tag{4}$$

$$R_r(\%) = \left(\frac{j_{w.2} - j_p}{j_{w.1}}\right) \times 100 \tag{5}$$

$$R_{ir}(\%) = \left(\frac{j_{w.1} - j_{w.2}}{j_{w.1}}\right) \times 100 = R_t - R_r \tag{6}$$

8. Oil Rejection

Oil-water emulsion (diesel oil, SAF 40) was prepared by heating the mixture at 30 °C under stirring (400 rpm) for 300 min. An emulsifier was not used in this case. The oil droplet size distribution was kept constant by a continuous stirring of the feed during the filtration. The concentrations of 300 and 500 ppm were used to

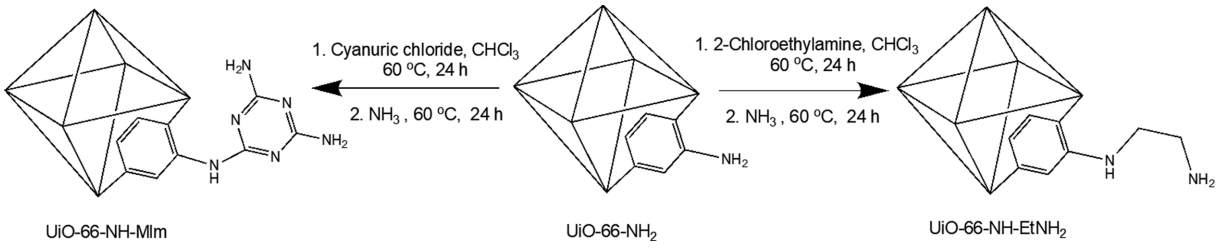

Fig. 1. Schematic procedures for the modification of UiO-66-NH_2 with ethylamine and melamine.

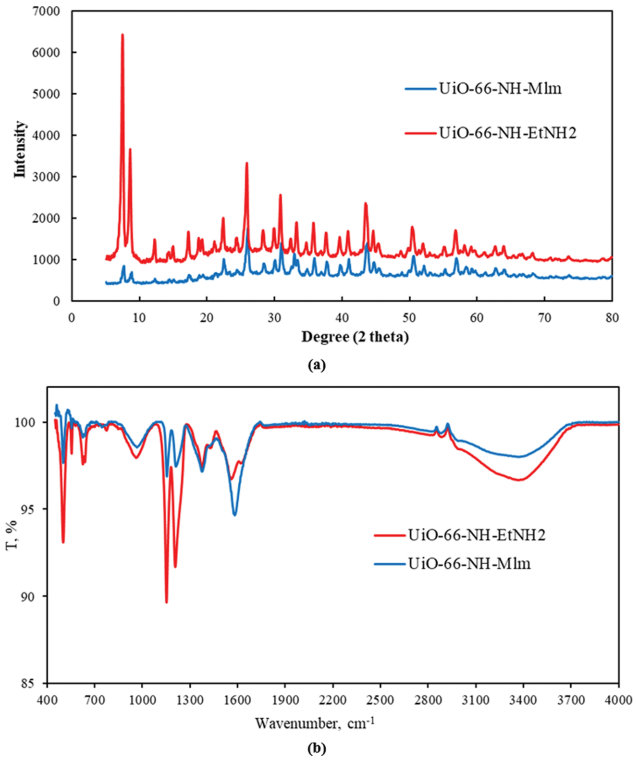

Fig. 2. XRD patterns (a) and FT-IR spectra (b) of the modified MOFs.

evaluate membrane rejection and performance.

RESULTS AND DISCUSSION

1. Preparation of Modified UiO-66-NH_2

UiO-66-NH_2 was modified through a solvothermal post-synthesis modification (PSM) by grafting chloroethylamine (to generate ethylenediamine, denoted UiO-66-NH-EtNH_2) and cyanuric chloride (to generate subsequently melamine, denoted UiO-66-NH-Mlm) (Fig. 1). The modified MOFs were characterized by different techniques such as XRD, ATR-IR, CHN, TGA, and BET. By introducing ethylamine to the framework, an additional primary amine with higher basicity was added to the structure, while the aromatic amine has low basicity. In melamine-grafted MOF, numerous amine groups on the melamine ring are available, which could provide hydrophilicity via hydrogen bonding.

Fig. 2(a) represents the XRD patterns of the modified MOFs. High similarity in the patterns of the modified MOFs with that in the parent MOF [34] indicates that the framework of the UiO66-

Table 2. Elemental analysis of the MOFs obtained by CHN

MOFs	CHN		
	N (%)	C (%)	H (%)
UiO-66-NH_2	5.58	26.16	1.66
UiO-66-NH-EtNH_2	5.84	29.46	3.48
UiO-66-NH-Mlm	11.51	34.4	3.06

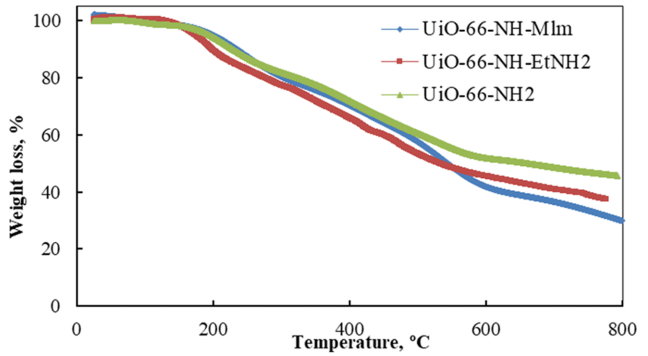

Fig. 3. TGA thermograms of the MOFs.

NH_2 [36] was maintained during the PSM. Such similarity was also observed for ATR-IR spectra (Fig. 2(b)) of the modified MOFs, although some peak shifts towards low frequency appeared for the modified MOFs. The characteristic vibrational bands corresponding to UiO-66-NH_2 were found, for example, primary amine (3,350 cm^{-1}), carbonyl (1,656 and 1,387 cm^{-1}), aromatic C=C (1,574, 1,541 and 1,432 cm^{-1}), C-N (1,258 cm^{-1}), N-H bending (766 cm^{-1}), and Zr-O (664, 537 and 479 cm^{-1}) [36,37]. The corresponding vibration bands of ethylamine (C-H) were observed at 2,957 cm^{-1} (asymmetric) and 2,870 cm^{-1} (symmetric).

To estimate the number of organic species loading on the UiO-66-NH_2 after the PSM, CHN, and TGA analyses were carried out. Table 2 exhibits the elemental composition of UiO-66-NH_2 after the modification. The amount of nitrogen and carbon of the parent MOF were accordingly increased with the loading of organic species. A high quantity of nitrogen was found for melamine due to the high number of amine groups in its structure. In TGA analysis (Fig. 3), additional mass losses of 6.82% and 17.71% were obtained after grafting ethylamine and melamine, respectively. Thus, there is a great agreement between mass loading and mass loss results obtained by CHN and TGA, respectively. Moreover, the TGA thermograms exhibited that the thermal stability of UiO-66-NH-Mlm was similar to that of UiO-66-NH_2 and higher than that

Table 3. BET-specific surface area and pore size/volume of the UiO-66-NH_2 and the modified MOFs

	UiO-66-NH_2	UiO-66-NH-EtNH_2	UiO-66-NH-Mlm
BET surface area ($m^2\ g^{-1}$)	1,260	600	290
Average pore size (nm)	3.8	3.0	3.2
Total pore volume ($cm^3\ g^{-1}$)	0.47	0.22	0.10

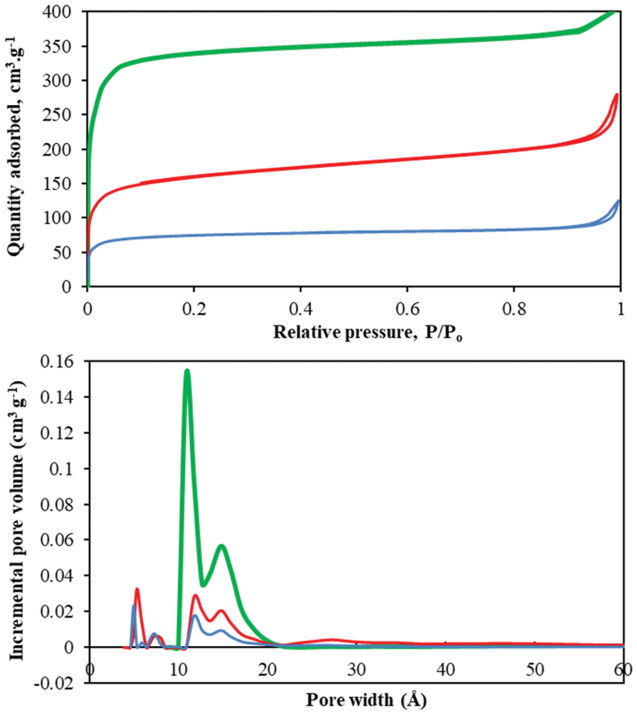

Fig. 4. N_2 adsorption-desorption isotherms and pore size/volume distributions of UiO-66-NH_2 (green), UiO-66-NH-EtNH_2 (red), and UiO-66-NH-Mlm (blue).

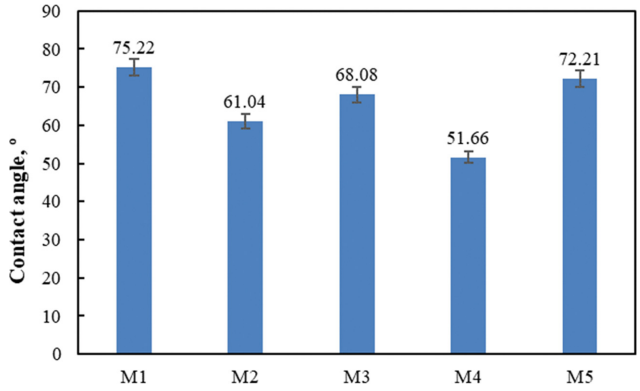

Fig. 5. WCA of the membranes.

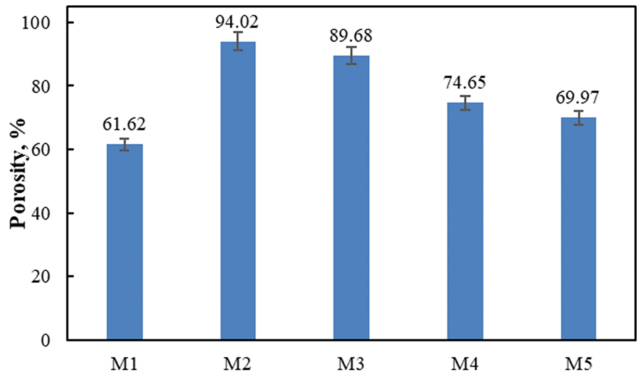

Fig. 6. Porosity measurement of the membranes.

of UiO-66-NH-EtNH_2. The first mass loss was observed at 170 °C for UiO-66-NH_2 and UiO-66-NH-Mlm, while this event was found at 130 °C for UiO-66-NH-EtNH_2.

The results of BET-specific surface area and porosity of the UiO-66-NH_2 and modified MOFs are given in Table 3. The surface area and the pore size/volume of the modified MOFs were significantly reduced upon modification. The quantity of reduction in the surface area and the porosity was related to the degree of modification, as by increasing the organic species loading to the MOF, more reduction in the pore size/volume occurred. Fig. 4 displays N_2 adsorption-desorption isotherms and pore size distributions of the MOFs. The presence of hysteresis in the isotherms showed a type IV isotherm, corresponding to the nature of mesoporous materials, while sharp gas adsorption at low pressure (i.e., P/P_o=0.02) revealed the behavior of microporosity in the MOF. Therefore, a combination of micro-and mesopores exists in the frameworks.

2. Membrane Hydrophilicity

Water contact angle (WCA) was regulated to examine the water that tends to spread on the membrane surface (Fig. 5). As expected, the wettability of the modified membranes increased (i.e., decreasing the WCA) by incorporating hydrophilic additives. Although the number of hydrophilic groups increased with increasing the number of additives (0.5 wt%), the hydrophilicity of the modified membranes was found to be decreased. It might be related to the possible agglomeration in higher additive loading, which prevents the migration of the additives toward the membrane surface (during the phase inversion). The formation of a porous sublayer can be another reason for this evidence (*cf.* Fig. 8).

3. Morphology Analysis

The effect of additive loading on the membrane porosity was studied. It is known that the membrane PWF is related to the membrane cavity and the pore size [38]. According to the porosity data (Fig. 6), the modified membranes, with different additive types and loadings, showed porosity improvement in comparison with the bare membrane. It is commonly understood that the addition of porous additives to the polymeric matrix affects the porosity of the resulting membrane. The membranes with modified additives showed higher porosities compared to the bare membrane. This effect was also notable for the membranes with additives having a larger structure of melamine (compared to ethylenediamine). It seems that the melamine ring occupies larger spaces around the

additive particles and subsequently generates additional porosity in the space of inter-particles. Furthermore, a higher porosity was observed for the membranes with lower additive loadings (0.1 wt%; M_2 and M_4). Although the addition of a high amount of additives in the membrane matrix increases the membrane cavity, the particle agglomeration is a limiting factor in higher loading and reduces the membrane porosity (M_3 and M_5). To find a direct correlation between the porosity and the behavior of the membranes, the permeation flux was examined, and the results are demonstrated in Fig. 7. As expected, by increasing the membrane porosity, the permeation water flux of the membranes was enhanced.

For further study on the membrane porosity, the SEM technique was employed to investigate the membrane cross-section (Fig. 8). A dense top layer was observed for the modified membranes with higher additive loading, 0.5 wt% in M_3 and M_5 (Fig. 8(c), (e)), which could be related to the higher viscosity of the casting solution. The high viscosity can reduce the rate and amount of additive migration toward the membrane surface during the phase inversion. The dense top-layer was reduced the membrane permeability and flux. In contrast, the membranes with low additive loading (M_2 and M_4) exhibited a porous top-layer and enhanced water permeability. Moreover, the flux increment could be related to the formation of an aquatic layer on the surface of the modified membrane (e.g.,

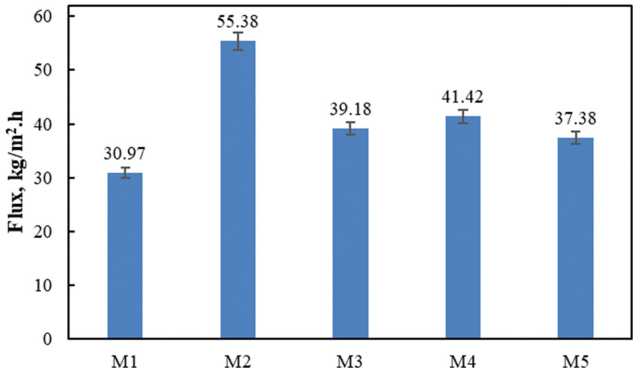

Fig. 7. The PWF of the membranes.

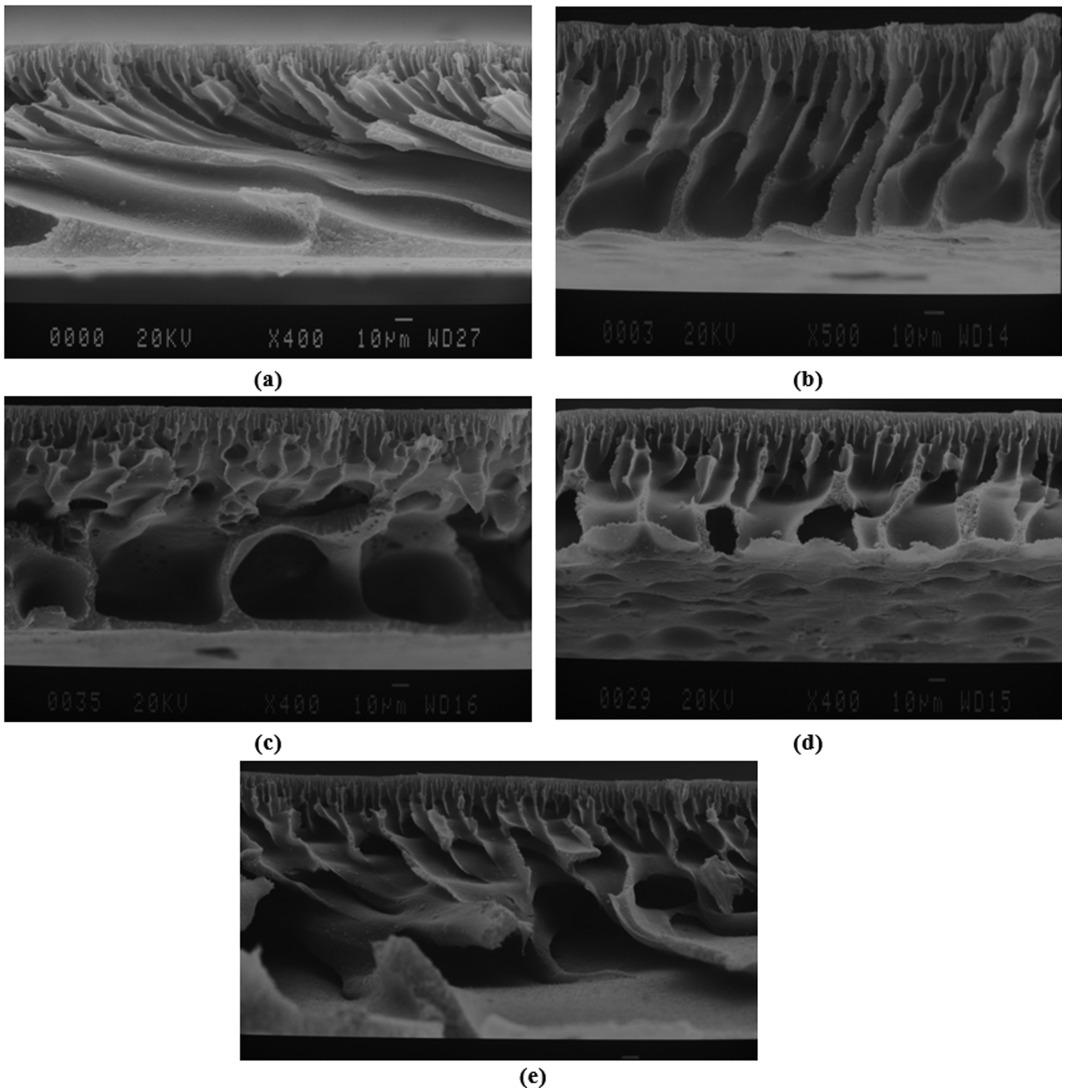

Fig. 8. SEM images of the membranes, (a) M_1, (b) M_2, (c), M_3, (d) M_4, and (e) M_5.

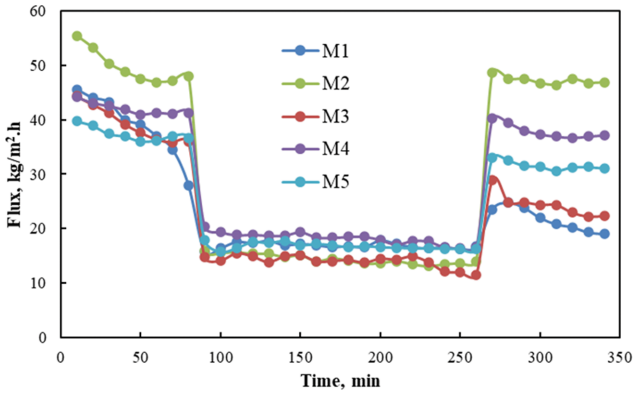

Fig. 9. Three-step experiment: (i) distilled water testing, (ii) milk powder testing (1,000 ppm), and (iii) distilled water testing.

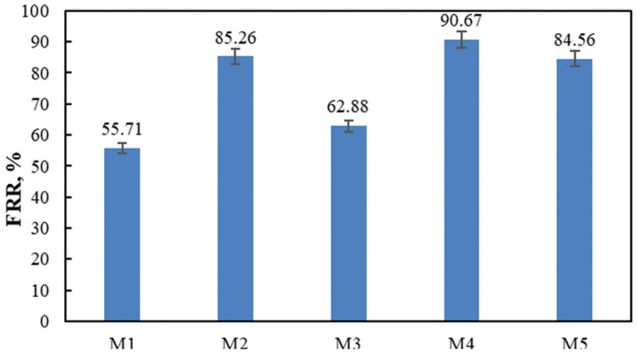

Fig. 10. FRR results of the membranes.

M_2), incorporated with melamine-modified MOF. Thus, the presence of more hydrophilic groups (-NH_2) in the modified MOFs facilitates the formation of the hydrophilic layer on the membrane surface.

4. Fouling Behavior

To evaluate the membrane behavior and reproductivity, the membranes were tested with milk powder solution as a model foulant. A three-step experiment, distilled water-milk powder-distilled water testings, was designed for this purpose (Fig. 9). All membranes showed almost the same trend in the three-step examination, which can be promising in membrane reproductivity and self-cleaning. The modified membranes, compared to the bare membrane, exhibited better water flux due to their greater porosities (Fig. 6). For M_2 and M_4 (0.1 wt% of the modified MOFs), the distilled water testing (before and after milk testing) did not show any reduction trend.

The flux recovery ratio (FRR) was also calculated, and the results are in Fig. 10. For M_2 and M_4, the recovery ratio ability was significant in comparison with others (>85%), due to an optimal additive percentage (0.1 wt%) in the modified membranes (absence of additive agglomeration). In addition, enhanced porosity and hydrophilicity in the modified membranes prevent the formation of a permanent cake layer (hydrophobic layer) on the surface and improve the water permeation.

To consider the membrane kinds of resistance, the reversible and irreversible resistances were calculated after the milk powder solution test (Fig. 11). The bare membrane showed the most irreversible resistance, which means a weak performance observed after a few frequent uses. In contrast, the modified membranes, M_2 and M_4, demonstrated the highest reversible resistance and the lowest irreversible resistance, respectively.

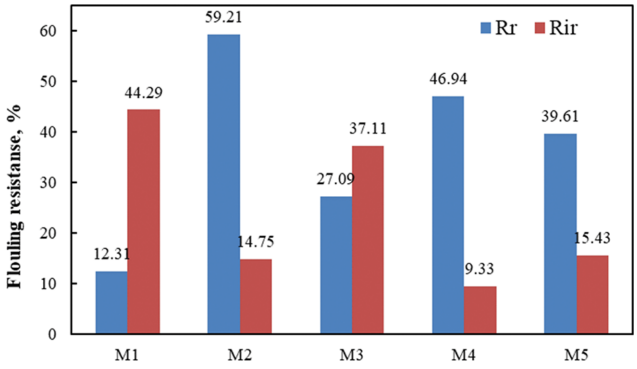

Fig. 11. Membrane reversible and irreversible fouling resistance.

Table 4. The surface roughness parameters for the prepared membranes

Membrane	S_a (nm)	S_q (nm)	S_z (nm)
M_1	16.182	21.292	215.78
M_2	0.977	1.184	3.645
M_3	3.188	3.610	7.995
M_4	1.195	1.575	4.587
M_5	4.685	5.651	13.006

For membranes with higher additive loading (M_3 and M_5), less resistance improvement was observed, which could be related to the presence of surface roughness. In the case of high roughness, foulant can be trapped between peaks and valleys of the membrane surface. The surface topography and the corresponding roughness of the membranes were studied by AFM (Fig. 12 and Table 4). The roughness of the bare membrane was significantly reduced after the introduction of the additives. The lowest roughness parameters (S_a, S_q, S_z) were observed for the membranes with an optimal additive loading of 0.1 wt% (M_2 and M_4). For M_3 and M_5, the higher roughness caused an increase in R_{ir} and a moderate in FRR (Fig. 10).

5. Long-term Performance of the Membranes

To assess the performance of the membranes for industrial applications, their operational stability and reusability were investigated. For this purpose, a long-term frequent analysis for distilled water and oily wastewater was designed. The bare and the modified membranes (M_2 and M_4) were tested consecutively with distilled water and oily feed (500 ppm) without membrane cleaning (Fig. 13). As can be seen, the bare membrane did not show an acceptable trend of reusability, which means the membrane pores have been blocked after three-cycle filtration. There are two possible reasons for this observation: (i) the hydrophobic nature of the membrane surface (M_1) tends to absorb oily foulant via the formation of the cake layer, and (ii) low porosity and narrow channels in the top layer of the bare membrane (Fig. 8, SEM images) enhance the chance of pore-blocking by suspended organic colloids in the oily feed. These results also proved the results of fouling resistance reli-

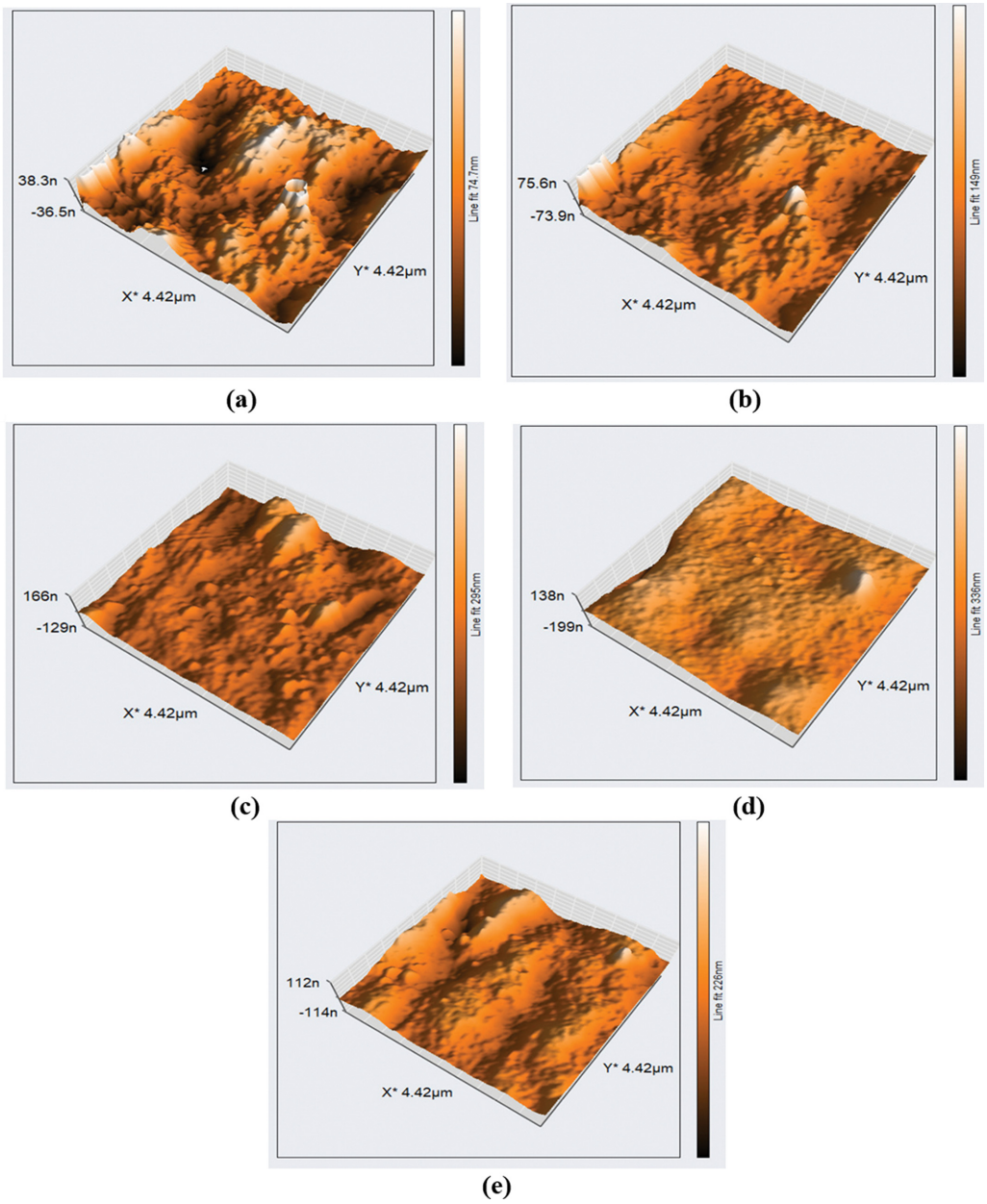

Fig. 12. AFM images of (a) M_1, (b) M_2, (c) M_3, (d) M_4, and (e) M_5.

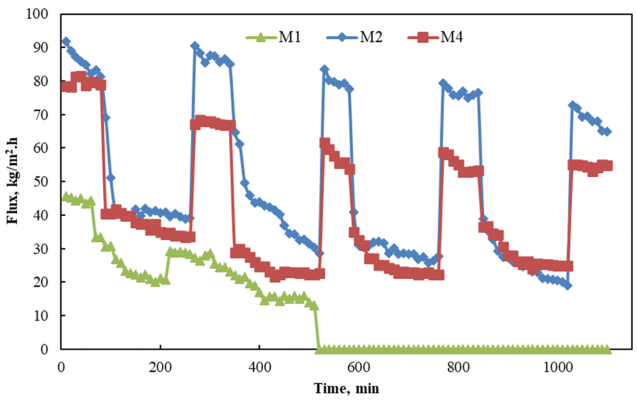

Fig. 13. Long-term filtration for the membranes.

ability. For the modified membranes, a reasonable performance was observed with seven consecutive cycles of distilled water/oily feed. The membrane (M_2), incorporated with melamine-modified MOF, showed better performance as melamine offers a large number of hydrophilic sites, which can have a positive impact on the membrane antifouling behavior and enhance the flux permeation via the formation of the hydration layer.

6. Membrane Stability

UiO-66-NH_2 is known as a high thermal/chemical stable MOF due to the presence of zirconium cores and aromatic ligands in its framework [39]. Therefore, the effect of MOF-based inorganic additives on the stability of the polymeric membrane was studied in harsh conditions (temperature and concentration). The operation (i.e., the three-step analysis) was tested at an elevated temperature

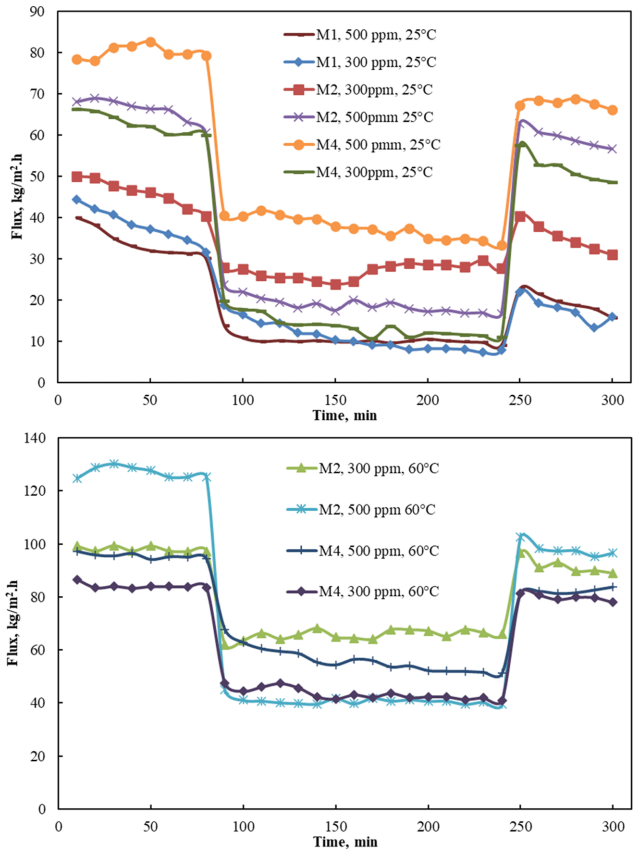

Fig. 14. Three-step analysis for simulated oily emulsion (500 and 300 ppm) in different temperature conditions (25 and 60 °C) for the bare and the modified membranes.

of 60 °C (compared to the room temperature) with feed concentrations of 300 and 500 ppm (Fig. 14). The modified membranes showed great performance in harsh conditions compared to the bare membrane. Better results were observed for the membrane M_2, and the highest performance was found in the feed concentration of 500 ppm (and also 300 ppm) at a high operating temperature of 60 °C. These results can be promising for industrial applications of modified MOF-based membranes.

7. Oil Rejection Test

The quality of the permeate after filtration of simulated oily wastewater by the modified membrane (M_4) was investigated by COD analysis. As can be seen in Fig. 15, a transparent liquid was obtained after the separation of water from the oil-water mixture with more than 99% oil rejection (obtained from the COD test).

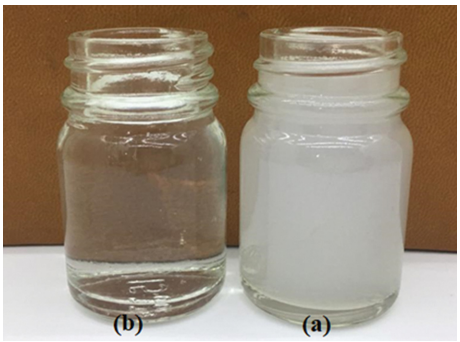

Fig. 15. Images of (a) oil-water emulsion feed (500 ppm oil concentration) and (b) the permeate after filtration with M_4.

CONCLUSION

Solvothermal post-modification of UiO-66-NH_2 was carried out with melamine and ethylamine. By modification, the number of amine groups on the structure of the parent MOF increased. These two modified MOFs were used for the fabrication of PES-based mix matrix membranes and subsequently employed for the separation of an oil-water mixture. As expected, the hydrophilicity of the modified membranes was enhanced by the introduction of modified MOFs possessing a high number of hydrophilic groups (-NH_2). The enhanced hydrophilicity of the modified membrane significantly improved the efficiency of oil/water filtration. In addition, the MOF additives enhanced the porosity and reduced the surface roughness of the modified membranes, which consequently improved the antifouling behavior. Long-term filtration performance and high thermal stability were also observed for the modified membranes. The thermal stability, efficient water permeation, and excellent reversible resistance can be attractive features of these MOF-based membranes for new applications in liquid-liquid separation and also gas separation.

DECLARATION OF INTERESTS

The authors declare that they have no known competing financial interests or personal relationships that could have appeared to influence the work reported in this paper.

The authors declare the following financial interests/personal relationships which may be considered as potential competing interests.

REFERENCES

1. P. Kumar, V. Bansal, K.-H. Kim and E. E. Kwon, *J. Ind. Eng. Chem.*, **62**, 130 (2018).
2. Y. Wang, B. Wang, Q. Wang, J. Di, S. Miao and J. Yu, *ACS Appl. Mater. Interfaces*, **11**, 1672 (2018).
3. Z. Xue, Y. Cao, N. Liu, L. Feng and L. Jiang, *J. Mater. Chem. A.*, **2**(8), 2445 (2014).
4. M. Schrope, *Nature*, **472**(7342), 152 (2011).
5. J. Lahann, *Nat. Nanotechnol.*, **3**(6), 320 (2008).
6. S. Kleindienst, J. H. Paul and S. B. Joye, *Nat. Rev. Microbiol.*, **13**(6), 388 (2015).
7. J. Fritt-Rasmussen, S. Wegeberg and K. Gustavson, *Water Air Soil Pollut.*, **226**(10), 1 (2015).
8. Q. Ma, H. Cheng, A. G. Fane, R. Wang and H. Zhang, *Small*, **12**(16), 2186 (2016).
9. S. Wang, K. Liu, X. Yao and L. Jiang, *Chem. Rev.*, **115**(16), 8230 (2015).
10. Z. Chu, Y. Feng and S. Seeger, *Angew. Chem. Int. Ed.*, **54**(8), 2328 (2015).
11. R. Miao, L. Wang, M. Zhu, D. Deng, S. Li, J. Wang, T. Liu and Y.

Lv, *Environ. Sci. Technol.*, **51**(1), 167 (2016).
12. M. Muthumareeswaran, M. Alhoshan and G. P. Agarwal, *Sci. Rep.*, **7**(1), 1 (2017).
13. Y. Zhu, D. Wang, L. Jiang and J. Jin, *NPG Asia Mater.*, **6**(5), e101 (2014).
14. H. Marioryad, A. M. Ghaedi, D. Emadzadeh, M. M. Baneshi, A. Vafaei and W. J. Lau, *ChemistrySelect*, **5**(6), 1972 (2020).
15. X. Fang, J. Li, X. Li, S. Pan, X. Zhang, X. Sun, J. Shen, W. Han and L. Wang, *Chem. Eng. J.*, **314**, 38 (2017).
16. Y. Ren, T. Li, W. Zhang, S. Wang, M. Shi, C. Shan, W. Zhang, X. Guan, L. Lv and M. Hua, *J. Hazard. Mater.*, **365**, 312 (2019).
17. Y.-X. Wang, Y.-J. Li, H. Yang and Z.-L. Xu, *J. Membr. Sci.*, **580**, 40 (2019).
18. W. Wang, L. Zhu, B. Shan, C. Xie, C. Liu, F. Cui and G. Li, *J. Membr. Sci.*, **548**, 459 (2018).
19. H. Fan, J. Gu, H. Meng, A. Knebel and J. Caro, *Angew. Chem., Int. Ed.*, **57**(15), 4083 (2018).
20. H. Liu, H. Yu, X. Yuan, W. Ding, Y. Li and J. Wang, *Chem. Eng. J.*, **374**, 1394 (2019).
21. Y. Shi, J. Huang, G. Zeng, W. Cheng, J. Hu, L. Shi and K. Yi, *Chemosphere*, **230**, 40 (2019).
22. F. Gholami, S. Zinadini, A. Zinatizadeh and A. Abbasi, *Sep. Purif. Technol.*, **194**, 272 (2018).
23. M. M. Baneshi, A. M. Ghaedi, A. Vafaei, D. Emadzadeh, W. J. Lau, H. Marioryad and A. Jamshidi, *Environ. Res.*, **183**, 109278 (2020).
24. J. Zhao, Y. Yang, C. Li and L.-a. Hou, *Sep. Purif. Technol.*, **209**, 482 (2019).
25. W. Lee, P. Goh, W. Lau, C. Ong and A. Ismail, *Sep. Purif. Technol.*, **214**, 40 (2019).
26. H. Furukawa, K. E. Cordova, M. O'Keeffe and O. M. Yaghi, *Sci.*, **341**(6149), 1230444 (2013).
27. J. Dechnik, J. Gascon, C. J. Doonan, C. Janiak and C. J. Sumby, *Angew. Chem. Int. Ed.*, **56**(32), 9292 (2017).
28. X. Li, Y. Liu, J. Wang, J. Gascon, J. Li and B. Van der Bruggen, *Chem. Soc. Rev.*, **46**(23), 7124 (2017).
29. S. Kitagawa, *Chem. Soc. Rev.*, **43**(16), 5415 (2014).
30. S. M. Maroofi and N. M. Mahmoodi, *Colloids Surf., A Physicochem. Eng. Asp.*, **572**, 211 (2019).
31. S. Zarghami, T. Mohammadi and M. Sadrzadeh, *J. Membr. Sci.*, **582**, 402 (2019).
32. J. Saththasivam, Y. Wubulikasimu, O. Ogunbiyi and Z. Liu, *J. Water Process. Eng.*, **32**, 100901 (2019).
33. J. Zhang, F. Zhang, A. Wang, Y. Lu, J. Li, Y. Zhu and J. Jin, *Langmuir*, **35**(5), 1682 (2018).
34. M. Samari, S. Zinadini, A. A. Zinatizadeh, M. Jafarzadeh and F. Gholami, *Sep. Purif. Technol.*, **251**, 117010 (2020).
35. M. J. Katz, Z. J. Brown, Y. J. Colón, P. W. Siu, K. A. Scheidt, R. Q. Snurr, J. T. Hupp and O. K. Farha, *ChemComm.*, **49**(82), 9449 (2013).
36. M. Kandiah, M. H. Nilsen, S. Usseglio, S. Jakobsen, U. Olsbye, M. Tilset, C. Larabi, E. A. Quadrelli, F. Bonino and K. P. Lillerud, *Chem. Mater.*, **22**(24), 6632 (2010).
37. J. H. Cavka, S. Jakobsen, U. Olsbye, N. Guillou, C. Lamberti, S. Bordiga and K. P. Lillerud, *J. Am. Chem. Soc.*, **130**(42), 13850 (2008).
38. Y. Li, S. Huang, S. Zhou, A. G. Fane, Y. Zhang and S. Zhao, *J. Membr. Sci.*, **556**, 154 (2018).
39. J. Cao, Y. Su, Y. Liu, J. Guan, M. He, R. Zhang and Z. Jiang, *J. Membr. Sci.*, **566**, 268 (2018).